SHIMADZU
Excellence in science

MO358

Life Science and Industrial Applications of the AXIMA Resonance

High Vacuum MALDI-QIT-TOF Mass Spectrometer

AXIMA Resonance

MALDI-QIT-TOF MS

High performance as standard...


Glycomics


Proteomics


Top-Down Proteomics


Non-Enzymatic / Chemical Modifications


Post-Translational Modifications


Small Molecules


Polymer Analysis


Lipidomics

...Results delivered

The AXIMA Resonance

Introduction

The AXIMA Resonance is a versatile MALDI mass spectrometer employed in a broad range of biological and organic analytical applications. Its main advantages are:

- True high-vacuum MALDI ion source
- Quadrupole ion trap with MS^n capability for structural elucidation
- High mass resolution and mass accuracy independent of the number of cycles during MS^n experiments
- Ability to isolate parent ions with isotopic resolution over a wide mass range - up to 1000 FWHM
- Variable energy CID control during acquisition
- Outstanding sensitivity - uncompromised design, to ensure highly efficient trapping functionality
- Low sample consumption - allowing many more MS^n experiments to be performed on the same spot
- Variable repetition rate N_2 laser
- Manual or fully automated operation allowing the seamless analysis of few or many samples as required
- Dedicated software solutions for a wide range of applications

Given these advantages, the AXIMA Resonance is ideally suited for high-end proteomics studies as well as less conventional studies with polymers, lipids and small molecules. The purpose of this document is to give an insight into the use of the AXIMA Resonance in these applications.

Glycomics

Classical glycan and glycopeptide analysis using MS^2 and MS^3

AXIMA Resonance, an ideal solution for carbohydrate research

Glycosylation is one of the major post-translational modifications (PTM) and has significant effects on protein folding and ultimately on protein activity. Identification of the glycan structure forms much of the challenge in this research field. However, of equal importance is the determination of the point of attachment to the protein. The AXIMA Resonance offers the advantage of being able to address both of these challenges.

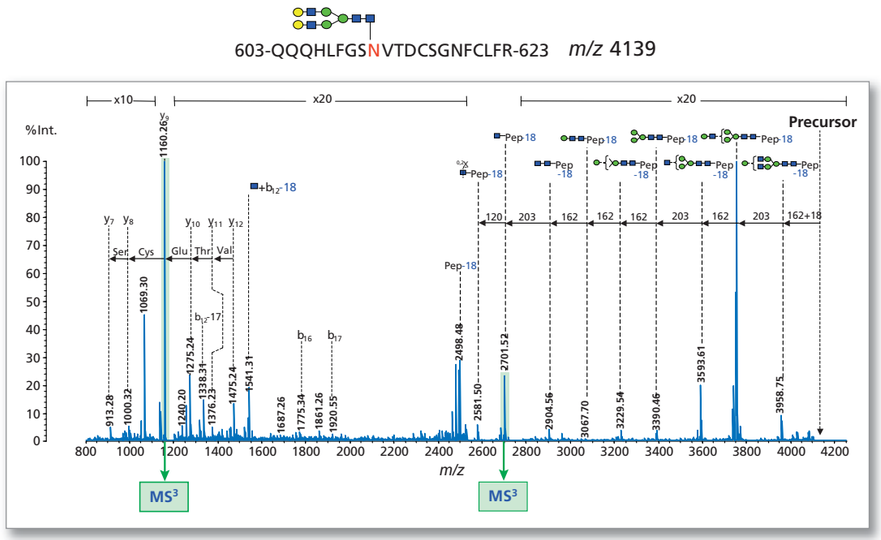

Figure 1: MS^2 spectrum of a human transferrin glycopeptide $[M+H-2Sia]^+$ (m/z 4139) that has already lost two sialic acid moieties. The spectrum exhibits the fragmentation of the glycan part attached to the peptide.

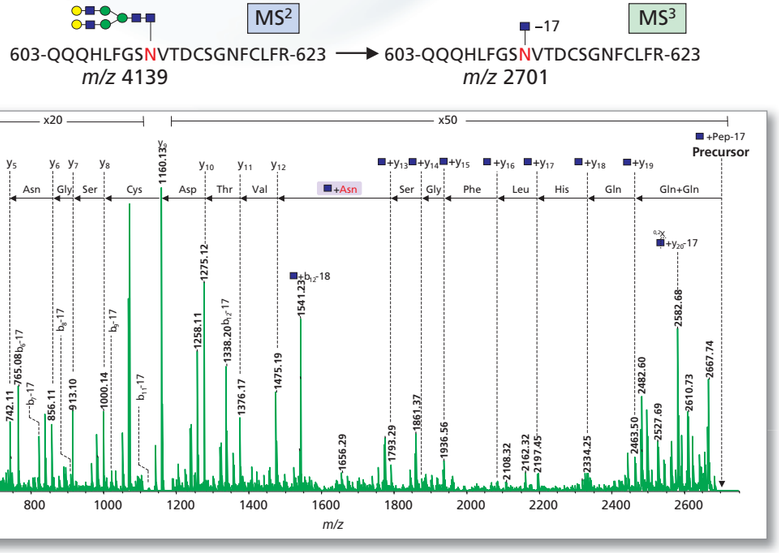

Figure 2: Positive ion MS^3 spectrum of the product ion at m/z 2701 (from the MS^2 analysis of m/z 4139 ion), exhibiting fragmentation of the peptide backbone. The detection of specific fragments allowed the identification of the glycosylation site.

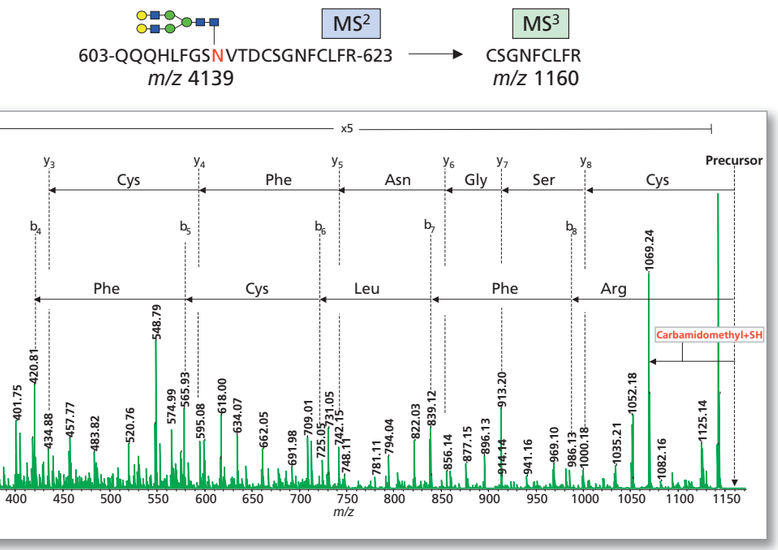

Figure 3: Positive ion MS^3 spectrum of the product ion at m/z 1160, exhibiting fragmentation of the peptide backbone. The peptide sequence is completely assigned.

Biosimilars

Accurate Glycan Analyser, a one-stop platform for smarter carbohydrate research

Accurate Glycan Analyser is a software-directed multistage MALDI mass spectrometric approach using the unique MS^n capability offered by the AXIMA Resonance and a populated database of real MS and MS^n glycan spectra, guiding the user through the process of structural analysis of glycans without requiring an expert level of knowledge.

Unlike others, the Accurate Glycan Analyser database is populated with glycans of high biological relevance, that have been enzymatically generated using the extensive glycogene know-how from the Japanese National Institute of Advanced Industrial Science and Technology. This recombinant technology-based approach is unique in this field and provides the researcher with a database of considerable added value.

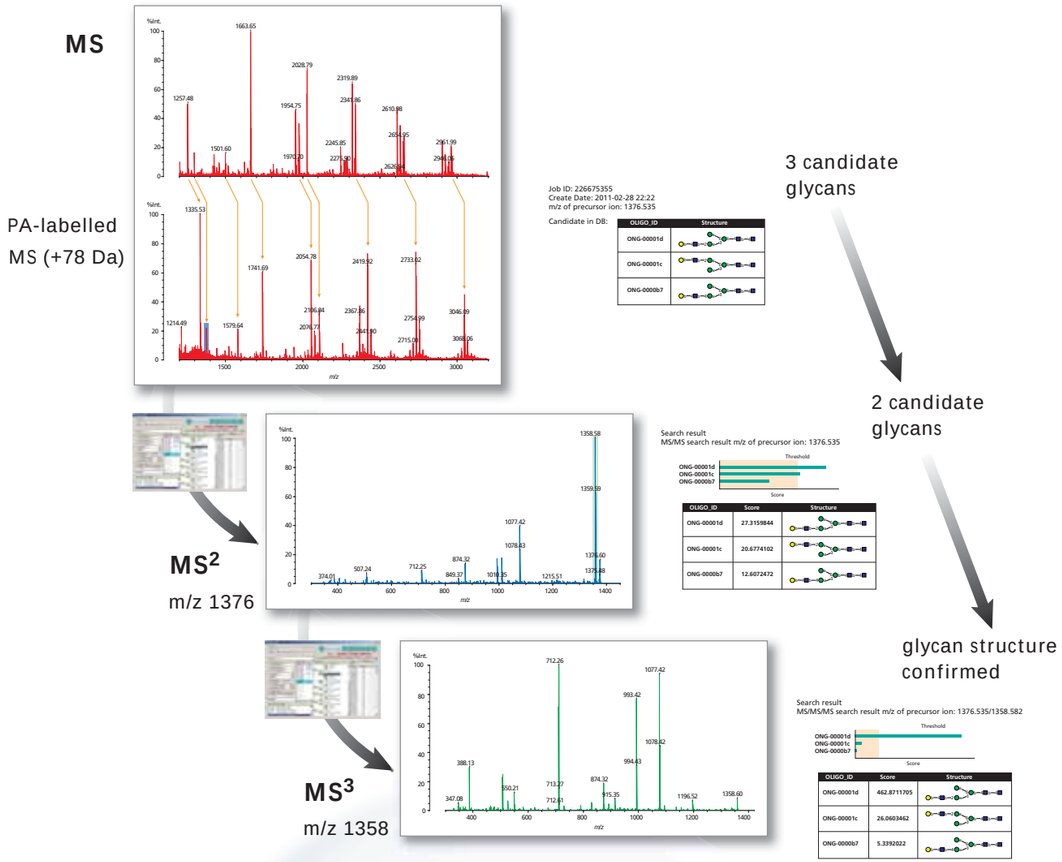

Figure 4: Overview of the Accurate Glycan Analyser - AXIMA Resonance workflow applied to PA-labelled glycans released from fetuin. At the MS level, potential glycan candidates are proposed. The software then suggests MS^2 precursor masses that can be analysed to confirm the proposed glycan structure. In some cases MS^2 alone is not sufficient to unequivocally identify a single glycan candidate, and thus the Accurate Glycan Analyser software proposes further MS^n precursor candidates (up to MS^4). For the fetuin example shown, MS^3 was necessary to unambiguously identify the glycan structure.

Human Factor IX (FIX), a single-chain glycoprotein, plays an important role in the intrinsic blood coagulation pathway and is used as a treatment for the bleeding disorder haemophilia B. There are two known glycosylation sites (Asn-157 and Asn-167).
The production of therapeutically active recombinant and plasma-derived FIX is approved and regulated by US and European agencies. The current regulatory levels of quality control require meticulous characterisation of the glycosylation pattern. However, due to the branched nature of glycans, the unambiguous identification of their structure is not trivial. The Accurate Glycan Analyser - AXIMA Resonance platform facilitates this identification.

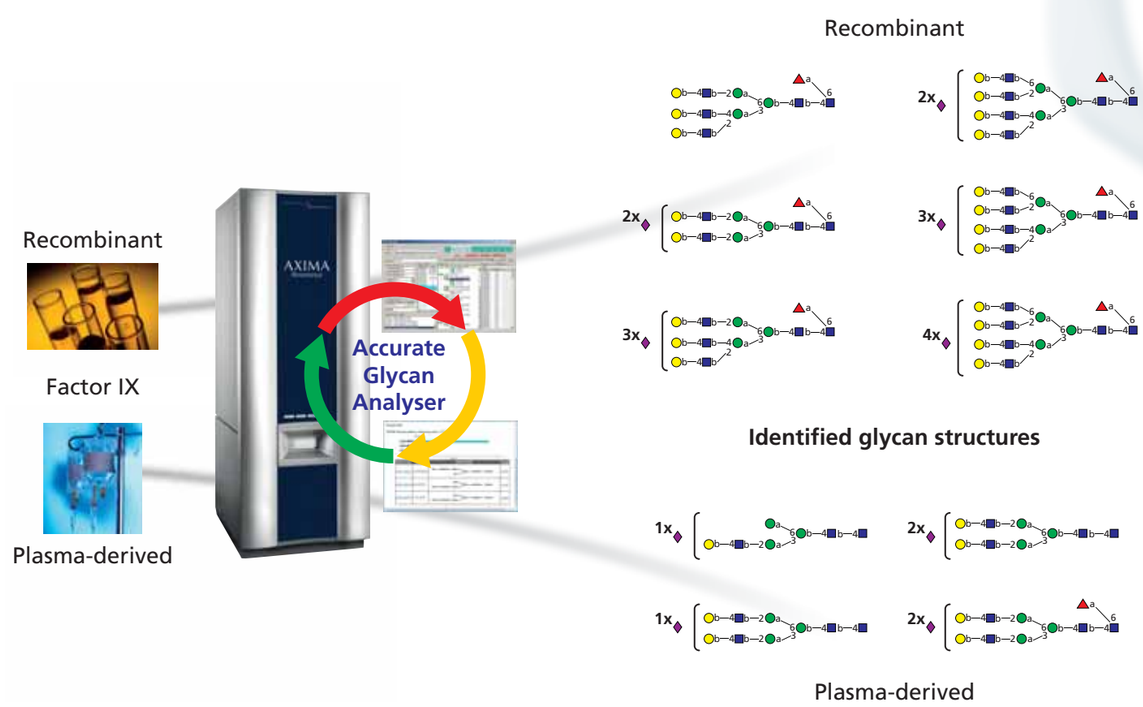

Figure 5: Summary of the identified glycan structures observed in plasma-derived and recombinant FIX using the Accurate Glycan Analyser software in combination with MS^n analyses. Significant differences were observed, in particular the extent of fucosylation and the core structures of the identified glycans.

Proteomics

Classical Proteomics

AXIMA Resonance, designed with sequencing and structural characterisation in mind

Peptide mass fingerprint (PMF) and MS^2 ion searching are widely used to enable high throughput protein identification. The example shown here illustrates the suitability of the AXIMA Resonance for classical proteomics applications. The proteins retained during a novel immunoadsorption therapy for rheumatoid arthritis (schematic 1) were studied in detail, combining 1D gel electrophoresis, PMF and MS^2 analysis.

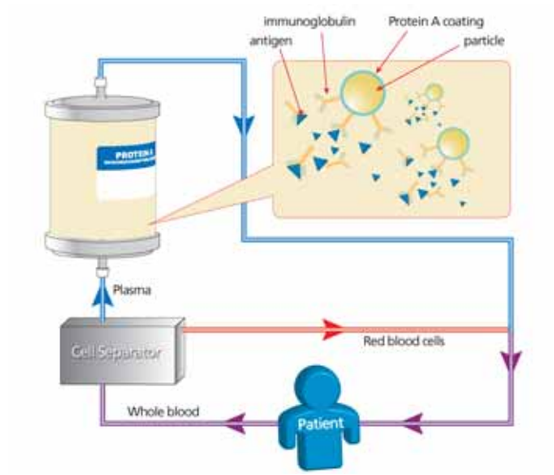

Schematic 1: Treatment schematic of Staphylococcal Protein-A based immunoadsorption therapy. The patient plasma is separated from the red blood cells, passed through the immunoadsorption column, recombined with the blood cells and returned to the patient. Immobilised Protein-A binds immunoglobulins and attached proteins (antigens).

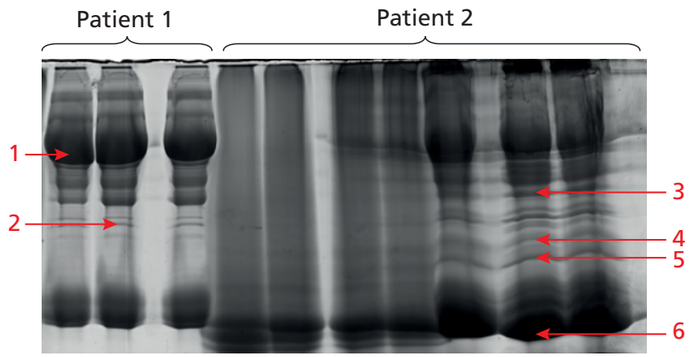

Figure 6: 1D SDS-PAGE of the proteins retained on column during immunoadsorption treatment of rheumatoid arthritis patients 1 and 2. Marked bands were excised and subjected to in-gel digestion with trypsin.

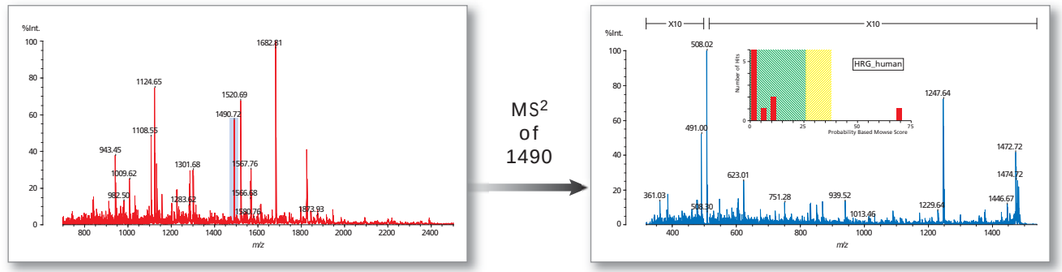

Figure 7: PMF mass spectrum of the tryptic digest of gel band 4 (left) and MS^2 analysis of m/z 1490 with individual Mascot MS^2 Ion Search (right) result.

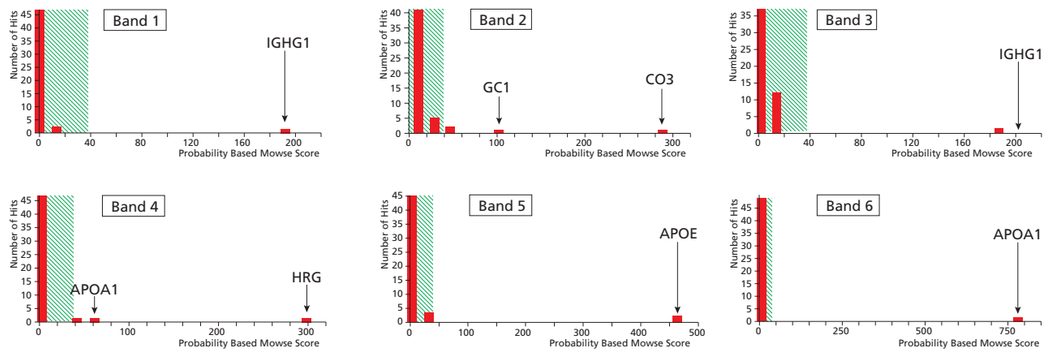

Figure 8: Summary of Mascot Ion Search results for all selected gel bands analysed for each patient. Matches to apolipoprotein A1 (APOA1), apolipoprotein E (APOE) and histidine-rich glycoprotein (HRG) were identified. Lipoprotein A1 has been reported in the literature to be present at an increased level in rheumatoid arthritis patients, however, little is understood of its biological role in inflammatory disease or the biological and therapeutic significance of the partial removal of these proteins from the bloodstream of rheumatoid arthritis sufferers.

Microbial Proteomics

Expanding rapid microbial identification through targeted proteomics

Mass spectrometric microbial identification is generally obtained using straightforward fingerprinting methods (eg: using the Saramis software on the AXIMA ID*plus* platform). However, the investigation of differences at the fingerprint level using MS^2 methods can provide more valuable and detailed information regarding the bacterial cells investigated.

The emergence of multi-drug resistant (MDR) enterobacteriaceae that can produce extended-spectrum beta-lactamases (ESBLs) is currently a major worldwide concern. These enzymes confer resistance to a wide spectrum of beta-lactam antibiotics currently used as first-line empirical therapy in the management of gram negative bacterial infections.

Significant differences in the microbial fingerprint were observed between ESBL- and non ESBL-producing *E. coli*. In particular, two peaks at m/z 2341.3 and m/z 3790.0 dominated the fingerprint from ESBL-producing *E. coli*. These potential biomarkers were selected for more in depth analysis by high resolution MS^2.

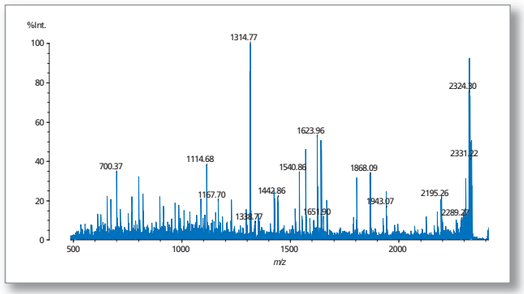

Figure 9: MS^2 mass spectrum of m/z 2341.

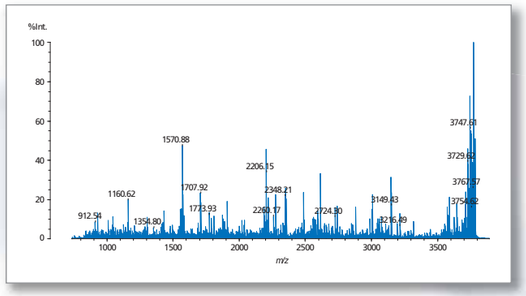

Figure 10: MS^2 mass spectrum of m/z 3790.

AAKKHHKNAKAEQKAPEQKAQ (m/z 2341)

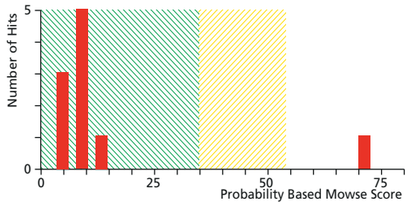

gi l 91210807 Mass: 11571 Score: 71 Queries matched: 1
acid shock protein precursor [Escherichia coli UTI89]

AETATTPAPTATTTKAAPAKTTHHKKQHKAAPAQKAQ (m/z 3790)

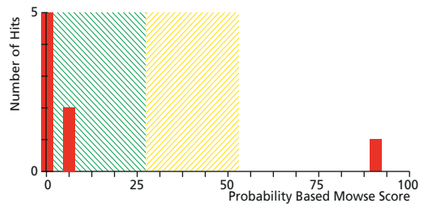

gi l 91210807 Mass: 11571 Score: 91 Queries matched: 1
acid shock protein precursor [Escherichia coli UTI89]

Figure 11: The MS^2 data were searched using Mascot Ion Search against all *E. coli* proteins in the NCBI database. Both peptides matched with high confidence to the same protein: acid shock protein precursor.

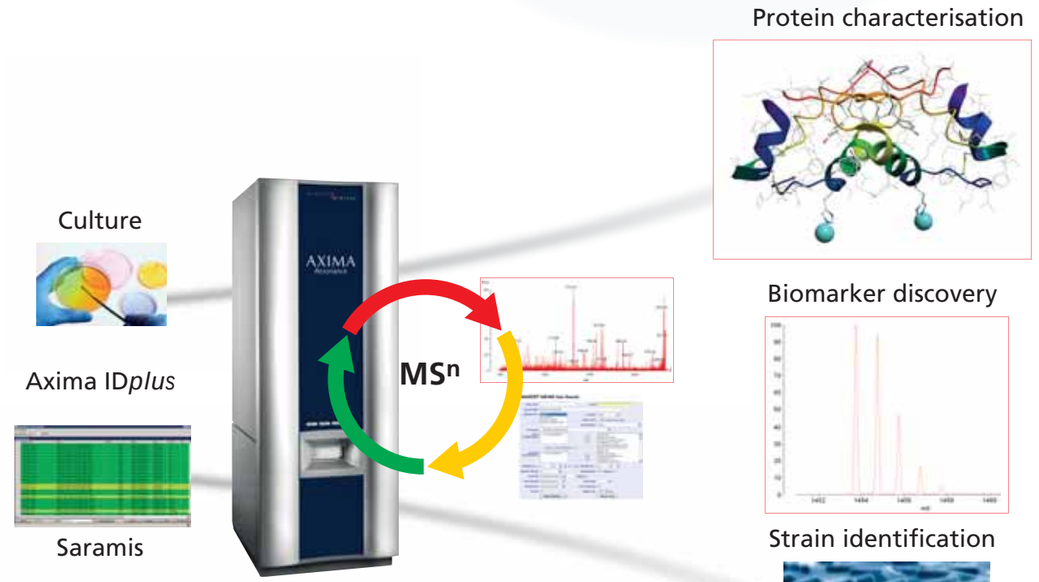

Top-Down Proteomics

Mapping intact proteins by combining In-Source Decay and MS^n

In-Source Decay (ISD) is a widely accepted technique in the sequencing of whole proteins by mass spectrometry, commonly referred to as top-down proteomics. Of particular importance is the characterisation of the protein N-terminus. Top-down sequencing using the AXIMA Resonance is achieved by a novel approach combining ISD and pseudo MS^n analyses in an ion trap. This has the advantage of desorbing large proteins and maintaining high resolution on the selection and detection of fragment ions.

ISD of human serum albumin provided a significant portion of the N-terminal sequence.

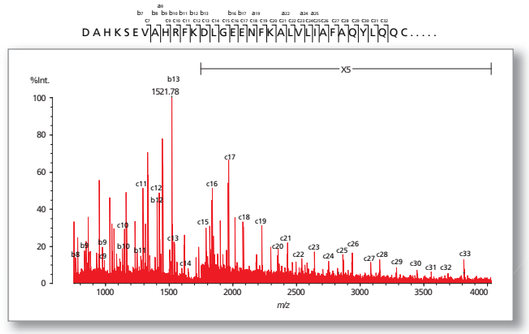

Figure 12: AXIMA Resonance ISD spectrum of HSA protein with its corresponding sequences. HSA protein gave a regular c-ion series from c7 to c33 and some b- and a-ion series. Observed mass resolution was greater than 11500 FWHM for the c33 ion.

Pseudo MS^3 and pseudo MS^4 fully characterised the N-terminus of the protein.

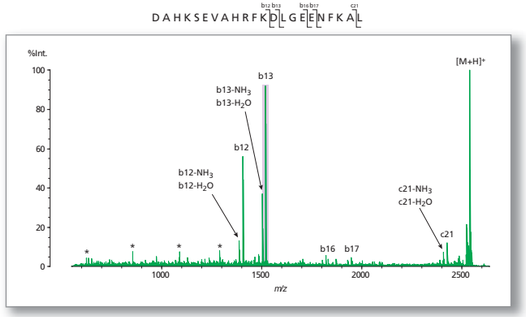

Figure 13: Pseudo MS^3 of the c22-ion (m/z 2540.30). The two main species correspond to b12 and b13 ions with their neutral losses of NH_3 and H_2O. Other species are annotated: b16, b17 and c21. The observed mass resolutions for b13 ion, b13- NH_3 and b13- H_2O exceeded 9000 FWHM. The asterisks "*" mark internal fragments.

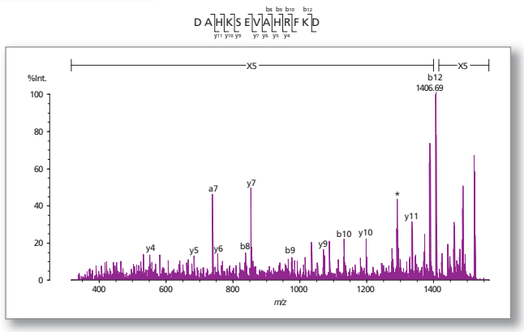

Figure 14: Pseudo MS^4 of the b13-ion (product ion of the c22-ion, m/z 1521.75). Many species were identified: b8-b10, b12, y4-y7 and y9-y11. Mass resolution was similar to the pseudo MS^3 spectrum.

Non-Enzymatic / Chemical Modifications

Thinking outside the box...
detecting protein modifications that are not in the database

Glycation is the non-enzymatic modification of a protein with a sugar molecule. Known as the Maillard reaction, it is the result of the condensation between the reducing end of a sugar and the reactive amine group of a protein. Unlike the enzyme-controlled glycosylation process, glycation is haphazard and tends to impair the function of the modified protein. Detailed characterisation of glycation products is therefore of high importance in the physiology and pathology of human diseases such as the chronic vascular complications of diabetes. It is also, however, relevant to the field of food processing.

In this study human serum albumin (HSA) glycation was investigated.

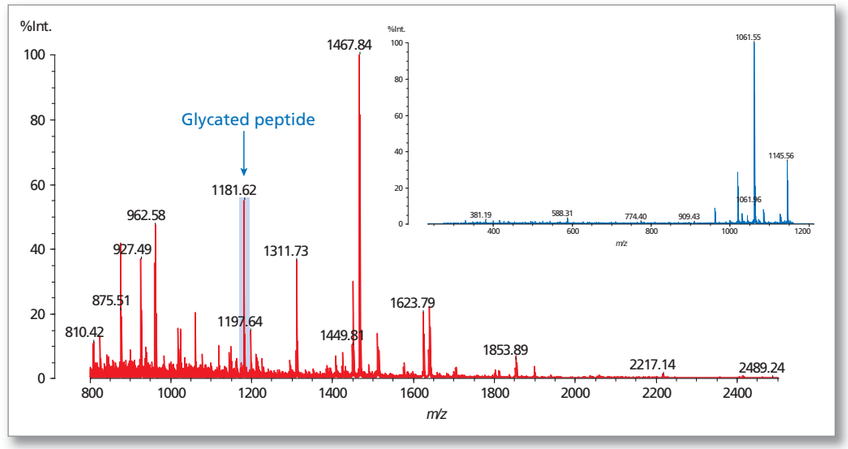

Figure 15: HSA was incubated with glucose for three weeks, digested with trypsin and the PMF was compared to that of unmodified HSA. Several differences between native and glycated HSA PMF were observed. These were analysed with MS^2, eg: MS^2 of m/z 1181 (inset).

PTMFinder is Shimadzu proprietary software that uses data mining to investigate protein modifications, including hypothetical and novel modifications. PTMFinder software offers the possibility of screening large MS^2 datasets for specific peptide modifications.

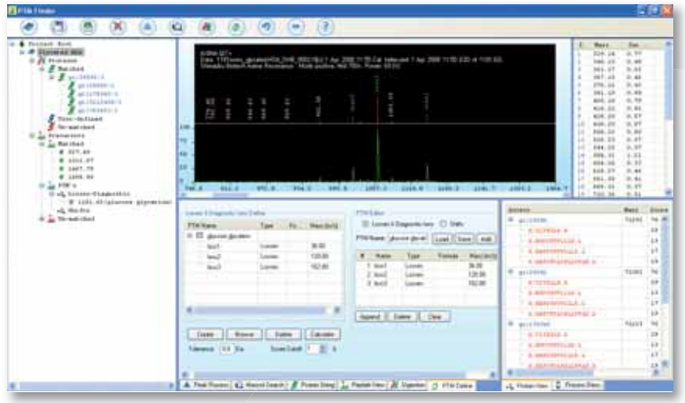

Figure 16: Glycation is a labile modification under UV MALDI conditions and in MS^2 produces a distinctive neutral loss pattern indicative of the modification (loss of 36, 120 and 162 Da from the precursor). Using the PTMFinder software, the specific MS^2 neutral loss signature for glucose was screened against glycated HSA digestion data. The screenshot illustrates the PTMFinder results highlighting the neutral losses on the spectrum.

Post-Translational Modifications

MS^n capability with high mass accuracy - an ideal alliance for post-translational modification analysis

Collagen is a highly abundant protein in mammals and constitutes the main protein within connective tissue, tendons, ligaments and skin. Hydroxylation is a common post-translational modification of collagen formed through the reaction of proline amino acid residues with prolyl hydroxylase. Alpha-1 type 1 collagen was investigated through enzymatic degradation and MS^n mass spectrometry. Several trypsin-digested peptides were found to contain multiple hydroxylation sites due to the prevalence of proline residues. Mass spectrometric elucidation of the exact location of hydroxylation sites was performed using the AXIMA Resonance mass spectrometer combining MS^2 and MS^3 for hydroxyproline (HyP) identification.

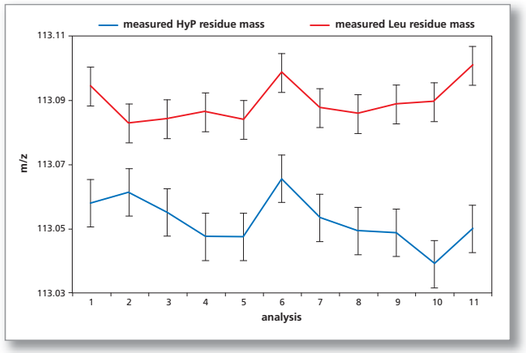

Figure 17: As HyP and Leu/Ile are isobaric in nominal mass (113.04768 and 113.08406 Da respectively), very high accuracy was necessary in order to specifically determine HyP sites. The accuracy of the AXIMA Resonance is sufficient to differentiate HyP from Leu/Ile (0.03638 Da) as illustrated in the statistical graph of multiple measurements of HyP (blue trace) and Leu/Ile (red trace) within HyP-Bradykinin and LHRH peptide sequences respectively.

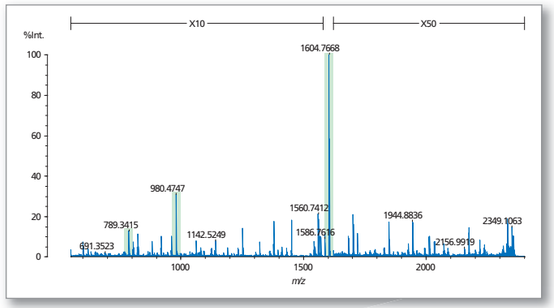

b	Seq	y
362.2341	G	
449.2661	S	2031.9843
546.3189	P	1944.9522
603.3404	G	1847.8995
674.3775	A	1790.8780
789.4044	D	1719.8409
846.4259	G	1604.8140
943.4786	P	1547.7925
1014.5158	A	1450.7397
1071.5372	G	1379.7026
1142.5743	A	1322.6811
1255.6220	HyP	1251.6440
1312.6435	G	1138.5963
1413.6912	T	1081.5749
1510.7439	P	980.5272
1567.7654	G	883.4744
1664.8182	P	826.4530
1792.8767	Q	729.4002
1849.8982	G	601.3416
1962.9823	I	544.3202
2034.0194	A	431.2361
2091.0408	G	360.1990
2219.0994	Q	303.1775
	R	175.1190

Figure 18: MS^2 spectrum of the proteolytic peptide GSPGADGPAGAPGTPGPQGIAGQR ((M+H)$^+$ = 2393 Da) from ITRAQ modified collagen alpha-1(I). The localisation of the HyP residue was demonstrated by a shift in the predicted y-ions (highlighted in yellow).

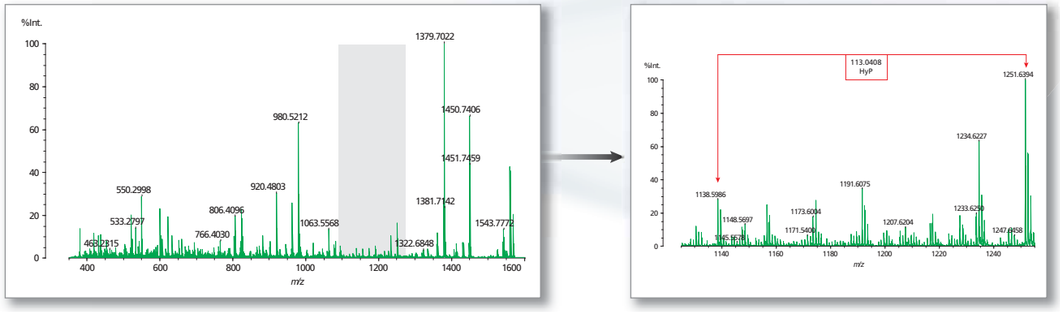

Figure 19: The dominant fragment ion at 1604 Da was selected for MS^3 analysis and this confirmed the location of the HyP residue.

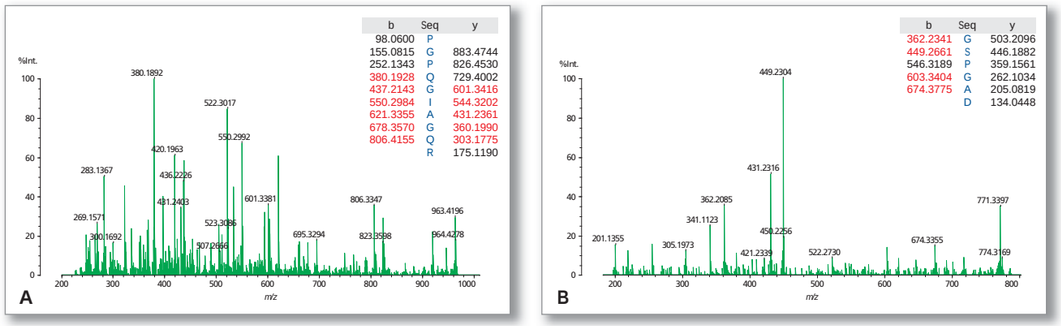

b	Seq	y
98.0600	P	
155.0815	G	883.4744
252.1343	P	826.4530
380.1928	Q	729.4002
437.2143	G	601.3416
550.2984	I	544.3202
621.3355	A	431.2361
678.3570	G	360.1990
806.4155	Q	303.1775
	R	175.1190

b	Seq	y
362.2341	G	503.2096
449.2661	S	446.1882
546.3189	P	359.1561
603.3404	G	262.1034
674.3775	A	205.0819
	D	134.0448

Figure 20: Combination of the MS^3 data for the fragment ions 980 Da (A) and 789 Da (B) with that of 1604 Da (Figure 19) provided the complete amino acid sequence for this peptide.

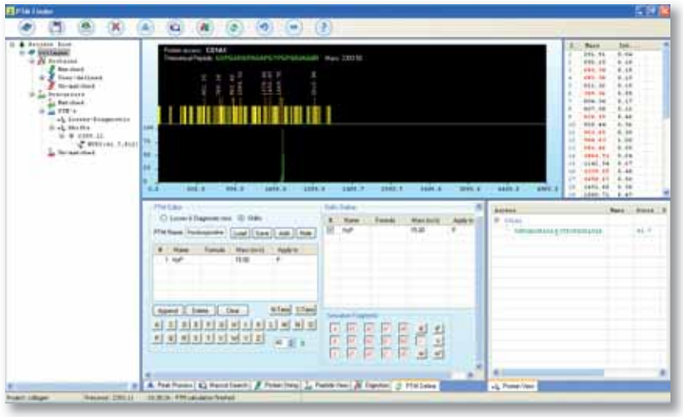

Figure 21: The MS^2 data were interrogated using PTMFinder software. Here hydroxyproline was defined as a possible modification of proline (ΔM = 15 Da) and the MS^2 of m/z 2393 was screened. A single HyP modification was correctly identified at amino acid position 12 out of the possible 5 proline sites within the peptide.

MS^n, maximising structural information for small molecules

Anthocyanins belong to the flavonoid group of polyphenolic compounds and have been investigated for multiple health benefits related to their anti-oxidant nature.

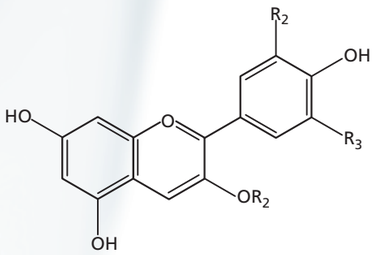

Anthocyanin	R1	R2	R3	Phenolic acid esters
Pelargonidin (Pg)	sugar moiety	H	H	*p*-coumaroyl
Cyanidin (Cy)		OH	H	
Peonidin (Pd)		OCH_3	H	caffeoyl
Delphinidin (Dp)		OH	OH	
Petunidin (Pt)		OCH_3	OH	feruloyl
Malvinidin (Mv)		OCH_3	OCH_3	

Figure 22: Basic structure of an anthocyanin. Many forms exist, the six most common core structures are shown in the table. The sugar moiety varies between mono-, di- and tri-saccharide units with various phenolic acid ester groups.

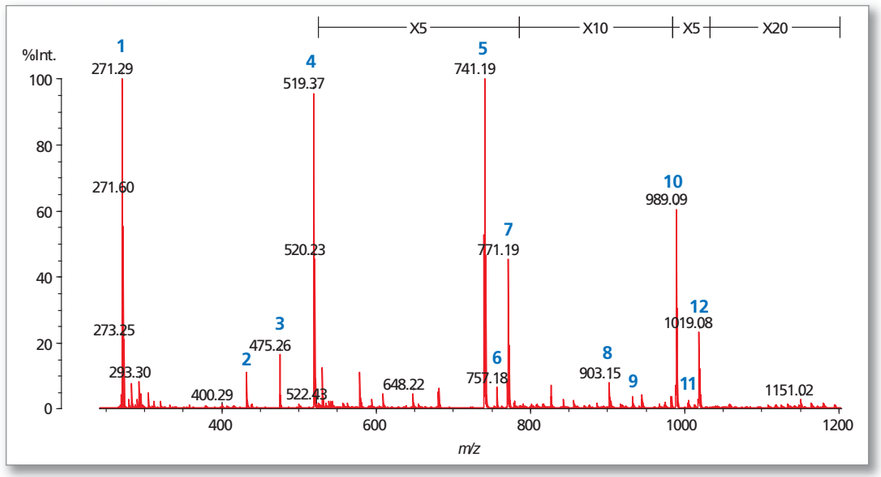

Figure 23: The MS spectrum of red radish extract contains a complex mixture of anthocyanins.

1 pelargonidin-aglycone
2 pelargonidin-3-glucoside
3 pelargonidin-3-glucoside acetylated
4 pelargonidin-3-(malonyl) glucoside
5 pelargonidin-3-(*p*-coumaroyl) diglucoside
6 pelargonidin-3-(caffeoyl) diglucoside
7 pelargonidin-3-(feruloyl) diglucoside
8 pelargonidin-3-(*p*-coumaroyl) diglucoside-5-glucoside
9 pelargonidin-3-(feruloyl) diglucoside-5-glucoside
10 pelargonidin-3-(*p*-coumaroyl) diglucoside-5-(malonyl) glucoside
11 pelargonidin-3-(caffeoyl) diglucoside-5-(malonyl) glucoside
12 pelargonidin-3-(feruloyl) diglucoside-5-(malonyl) glucoside

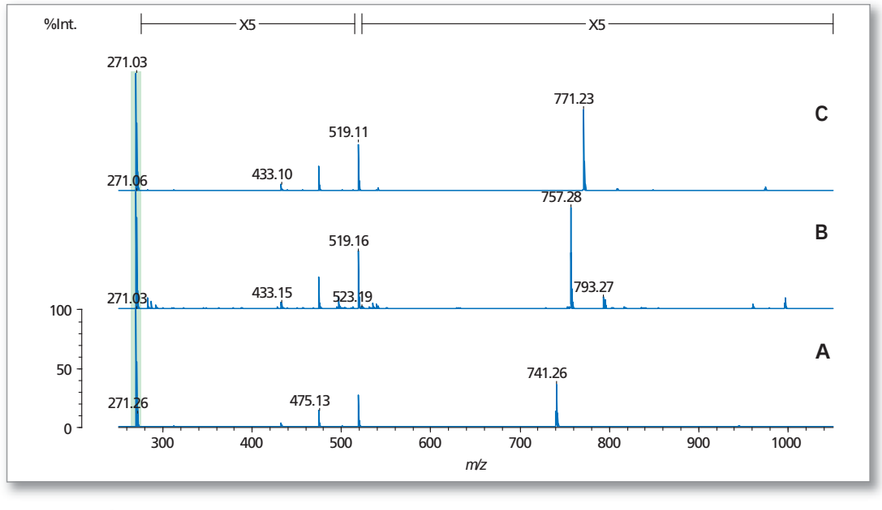

Figure 24: MS^2 analysis of three of the radish anthocyanins (m/z 989 (A), m/z 1005 (B) and m/z 1019 (C)) indicates that the fragmentation pathway mainly consists of the loss of the sugar moieties: loss of malonyl (86 Da), of 5-(malonyl) glucoside (248 Da), of the modified diglucosides at position 3, of both the modified diglucosides and malonyl and finally complete loss of all the sugar moieties to form the Pg-aglycone.

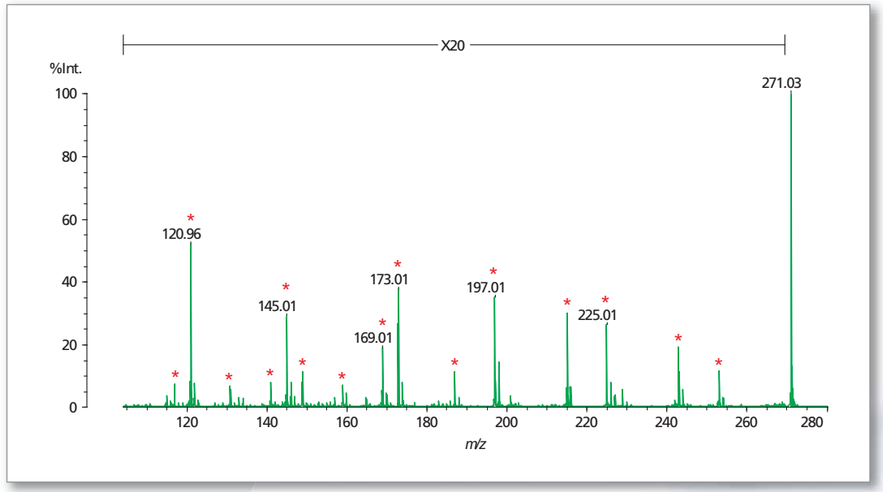

Figure 25: MS^3 analysis of the Pg-aglycone fragment ion (m/z 271). Each of the peaks annotated with * corresponds to a known fragment of the Pg-aglycone structure. Fragmentation proceeds through loss of water (18 Da), loss of CO (28 Da) and loss of acetyl (42 Da).

Polymers

Broadening horizons...

compositional analysis of synthetic polymers

Fatty alcohol alkoxylates are used as non-ionic surfactants in home and industrial cleaning agents. Characterised by important properties such as foam suppression, foam control and wetting effects, fatty alcohol alkoxylates are synthesised by reaction of fatty alcohols with alkoxides such as ethylene oxide and propylene oxide amongst others. Alkoxylates are also relevant in a broad range of chemical industrial applications where they are used as dispersal agents and emulsifiers.

MS and MS^2 were used to characterise the fatty alcohol alkoxylate polymer shown in schematic 2.

octanol-ethoxylate

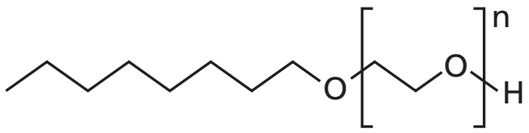

Schematic 2: Structure of the fatty alcohol alkoxylate polymers analysed.

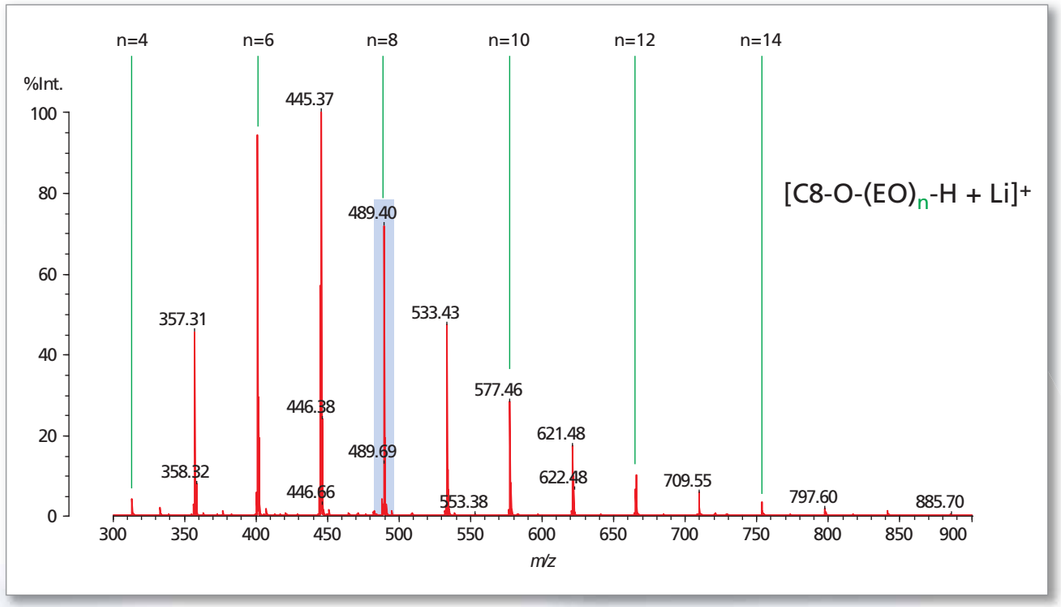

Figure 26: AXIMA Resonance mass spectrum of the ethoxylated octanol. The peaks represent $(M+Li)^+$ ions. The mass distribution in the spectrum is asymmetric due to the low degree of ethoxylation in this product.

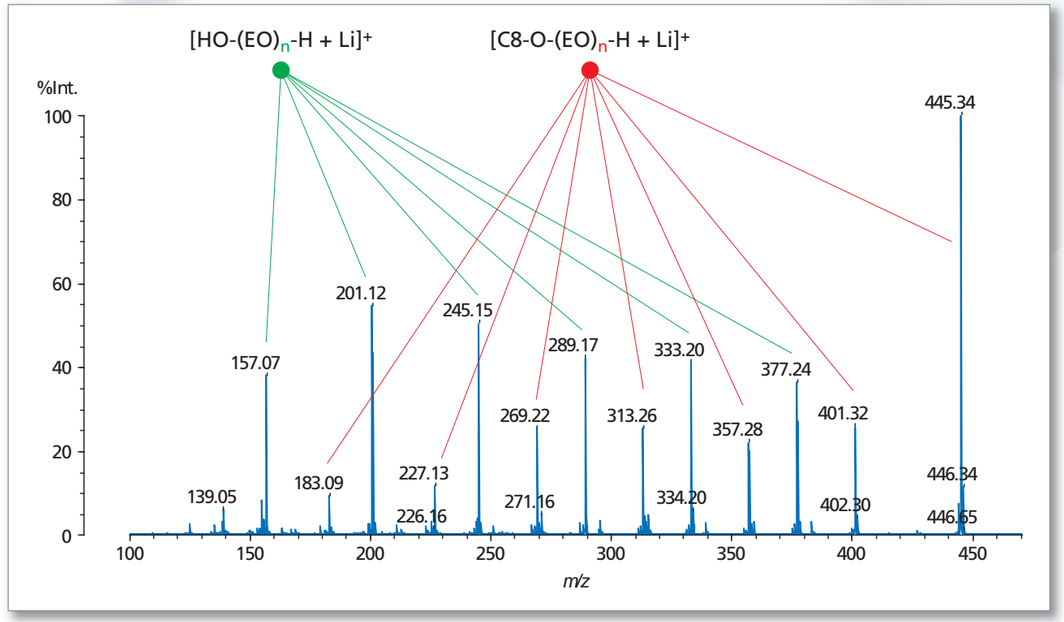

Figure 27: A key advantage of the AXIMA Resonance system is the ability to control the relative collision energy which results in high-quality CID-MS^2 spectra. This is the MS^2 spectrum of the lithium adduct precursor ion m/z 489 clearly showing the fragment series $[HO-(EO)_n-H+Li]^+$ and $[C8-O-(EO)_n-H+Li]^+$ (C8 = C_8H_{17} and EO= CH_2CH_2O).

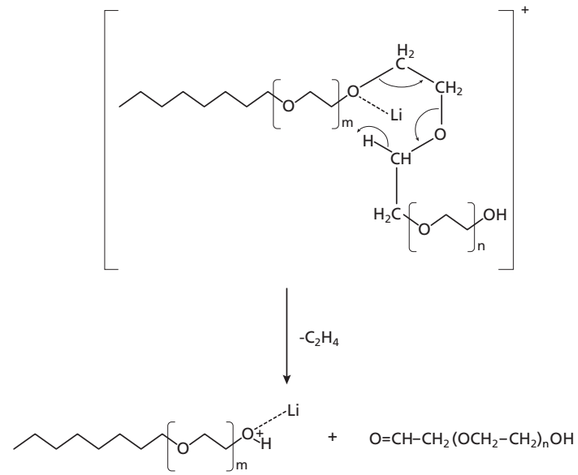

Schematic 3: A theory for the fragmentation of the ethoxylated fatty alcohols is based on the rearrangement reaction in which the lithium ion is attached in a transition state to the terminal oxygen. In the next step the elimination of ethylene takes place.

Lipidomics

Revolutionising lipid research with mono-isotopic precursor ion selection and MS^n capability

Lipids represent an important class of compound due to their broad range of vital biological functions. Mono-isotopic selection of lipids during MS^2 analysis is critical due to the natural occurrence of C-C bond unsaturation giving rise to ions that are separated by 2 Da in the mass spectrum.

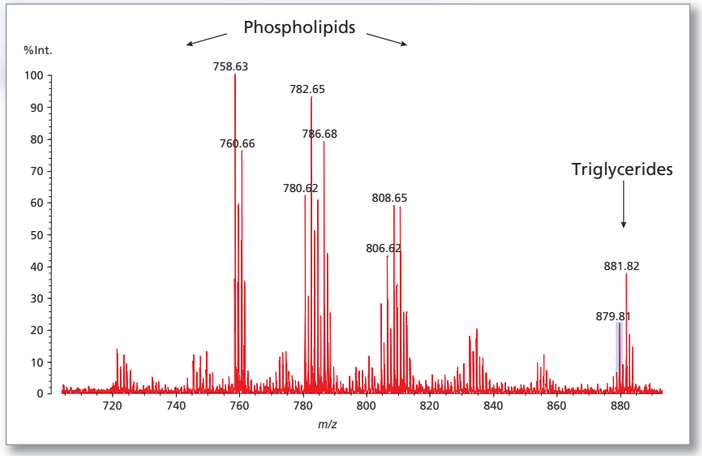

Figure 28: Representation of a typical MALDI mass spectrum of a crude mixture of lipids derived from human plasma. Plasma lipid extracts in MALDI-TOFMS exhibit mostly phospholipids and triacylglycerols (triglycerides or TAG). Depending on the experimental conditions (matrix used, solvent, cations, etc) it is possible to selectively ionise certain classes of lipids individually from a mixture. In this case, the chosen conditions allowed for the detection of mainly the phosphatidylcholine and TAG species.

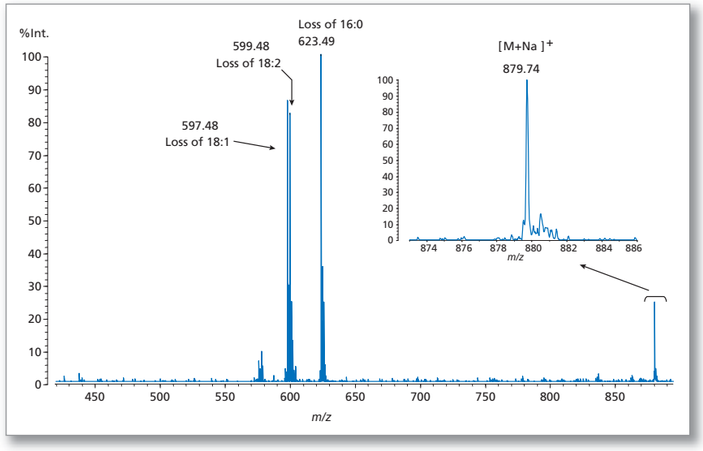

Figure 29: The positive ion MS^2 spectrum of a TAG (16:0, 18:2, 18:1) is shown. The sodium adduct $[M+Na]^+$ (m/z 879.74) was detected and selected for MS^2 with isotopic resolution in order to perform the CID experiment. The product ion spectrum clearly exhibits the loss of the three different fatty acid chains (loss of RCOOH) where RCOOH can be a 16:0, 18:1 or 18:2 fatty acid.

References

Ismail MN, Stone EL, Panico M, Lee SH, Luu Y, Ramirez K, Ho SB, Fukuda M, Marth JD, Haslam SM, Dell A. High Sensitivity O-glycomic Analysis of Mice Deficient in Core 2 {beta}1,6-N-acetylglucosaminyltransferases. *Glycobiology*. 2011 Jan; 21(1): 82-98.

Wada Y, Dell A, Haslam SM, Tissot B, Canis K, Azadi P, Bäckström M, Costello CE, Hansson GC, Hiki Y, Ishihara M, Ito H, Kakehi K, Karlsson N, Hayes CE, Kato K, Kawasaki N, Khoo KH, Kobayashi K, Kolarich D, Kondo A, Lebrilla C, Nakano M, Narimatsu H, Novak J, Novotny MV, Ohno E, Packer NH, Palaima E, Renfrow MB, Tajiri M, Thomsson KA, Yagi H, Yu SY, Taniguchi N. Comparison of methods for profiling O-glycosylation: Human Proteome Organisation Human Disease Glycomics/Proteome Initiative multi-institutional study of IgA1. *Mol. Cell Proteomics*. 2010 Apr; 9(4): 719-27.

Inagaki M, Nakaya S, Nohara D, Yabe T, Kanamaru Y, Suzuki T. The multiplicity of N-glycan structures of bovine milk 18 kda lactophorin (milk GlyCAM-1). *Biosci. Biotechnol. Biochem*. 2010; 74(2): 447-50.

Kasai H, Tsubuki M, Shimada K, Nambara T, Honda T. Analyses of biologically active steroids: antitumor active OSW-1 and cardiotonic marinobufotoxin, by matrix-assisted laser desorption/ionization quadrupole ion trap time-of-flight tandem mass spectrometry. *Chem. Pharm. Bull. (Tokyo)*. 2009 Sep; 57(9): 948-56.

Amano J, Sugahara D, Osumi K, Tanaka K. Negative-ion MALDI-QIT-TOFMS^n for structural determination of fucosylated and sialylated oligosaccharides labeled with a pyrene derivative. *Glycobiology*. 2009 Jun; 19(6): 592-600.

Amano J, Osanai M, Orita T, Sugahara D, Osumi K. Structural determination by negative-ion MALDI-QIT-TOFMS^n after pyrene derivatization of variously fucosylated oligosaccharides with branched decaose cores from human milk. *Glycobiology*. 2009 Jun; 19(6): 601-14.

Larsen MR, Trelle MB, Thingholm TE, Jensen ON. Analysis of posttranslational modifications of proteins by tandem mass spectrometry. *Biotechniques*. 2006; 40: 790-797.

Kameyama A, Kikuch N, Nakaya S, Ito H, Sato T, Shikanai T, Takahashi Y, Takahashi K, Narimatsu H. A Strategy for Identification of Oligosaccharide Structures Using Observational Multistage Mass Spectral Library. *Anal. Chem*. 2005; 77: 4719-4725.

Ito H, Kameyama A, Sato T, Sukegawa M, Ishida H, Narimatsu H. Strategy for the fine characterization of glycosyltransferase specificity using isotopomer assembly. *Nature Methods*. 2007; 4(7): 577-582.

Suzuki Y, Miyasaki M, Ito E, Suzuki M, Yamashita T, Taira H, Suzuki A. Structural Characterization of N-Glycans of cauxin by MALDI-TOF Mass Spectrometry and Nano LC-ESI-Mass Spectrometry. *Biosci. Biotechnol. Biochem*. 2007; 71: 811-816.

Zehl M, Pittenauer E, Jirovetz L, Bandhari P, Singh B, Kaul VK, Rizzi A, Allmaier G. Multistage and Tandem Mass Spectrometry of Glycosylated Triterpenoid Saponins Isolated from Bacopa monnieri: Comparison of the Information Content Provided by Different Techniques. *Anal. Chem*. 2007; 79: 8214-8221.

Takemori N, Komori N, Matsumoto H. Highly sensitive multistage mass spectrometry enables small-scale analysis of protein glycosylation from two-dimensional polyacrylamide gels. *Electrophoresis*. 2006; 27: 1394–1406.

Suzuki Y, Suzuki M, Nakahara Y, Ito Y, Ito E, Goto N, Miseki K, Iida I, Suzuki A. Structural Characterization of Glycopeptides by N-terminal Protein Ladder Sequencing. *Anal. Chem*. 2006; 78: 2239-2243.

Ojima N, Masuda K, Tanaka K, Nishimura O. Analysis of neutral oligosaccharides for structural characterization by matrix-assisted laser desorption/ionization quadrupole ion trap time-of-flight mass spectrometry. *J. Mass Spectrom*. 2005; 40: 380-388.

Fukuyama Y, Nakaya S, Yamazaki Y, Tanaka K. Ionic Liquid Matrixes Optimized for MALDI-MS of Sulfated/Sialylated/Neutral Oligosaccharides and Glycopeptides. *Anal. Chem*. 2008; 80: 2171-2179.

Nicolaou A, Kokotos G. Bioactive Lipids. Oily Press, Bridgwater, 2004.

Zhao N, Yao J. Characterization and sequence identification of angiotensin II by a novel method involving ultra-fast liquid chromatography assay coupled with matrix-assisted laser desorption/ionization quadrupole ion trap time-of-flight five tandem mass spectrometry analysis. *European Journal of Mass Spectrometry*. 2010; 16,6: 663–671.

Li Z, Leung W, Yon A, Nguyen J, Perez VC, Vu J, Giang W, Luong LT, Phan T, Salazar KA, Gomez SR, Au C, Xiang F, Thomas DW, Franz AH, Lin-Cereghino J, Lin-Cereghino GP. Secretion and proteolysis of heterologous proteins fused to the Escherichia coli maltose binding protein in Pichia pastoris. *Protein Expr. Purif*. 2010 Jul; 72(1): 113-24.

Sun LC, Yoshida A, Cai QF, Liu GM, Weng L, Tachibana K, Su WJ, Cao MJ. Mung Bean Trypsin Inhibitor Is Effective in Suppressing the Degradation of Myofibrillar Proteins in the Skeletal Muscle of Blue Scad (Decapterus maruadsi). *J. Agric. Food Chem*. 2010; 58(24): 12986-92.

Mecklenburg KL, Takemori N, Komori N, Chu B, Hardie RC, Matsumoto H, O'Tousa JE. Retinophilin is a light-regulated phosphoprotein required to suppress photoreceptor dark noise in Drosophila. *J. Neurosci*. 2010 Jan 27; 30(4): 1238-49.

Kruger AJ, Yang C, Tam SW, Hinerfeld D, Evans JE, Green KM, Leszyk J, Yang K, Guberski DL, Mordes JP, Greiner DL, Rossini AA, Bortell R. Haptoglobin as an early serum biomarker of virus-induced autoimmune type 1 diabetes in biobreeding diabetes resistant and LEW1.WR1 rats.
Exp. Biol. Med. (Maywood). 2010 Nov; 235(11): 1328-37.

Montgomery H, Tanaka K, Belgacem O. Glycation pattern of peptides condensed with maltose, lactose and glucose determined by ultraviolet matrix-assisted laser desorption/ionization tandem mass spectrometry.
Rapid Commun. Mass Spectrom. 2010 Mar; 24(6): 841-8.

Zhao L, Almaraz RT, Xiang F, Hedrick JL, Franz AH. Gas-phase scrambling of disulfide bonds during matrix-assisted laser desorption/ionization mass spectrometry analysis.
J. Am. Soc. Mass Spectrom. 2009 Sep; 20(9): 1603-16.

Tawaratsumida K, Furuyashiki M, Katsumoto M, Fujimoto Y, Fukase K, Suda Y, Hashimoto M. Characterization of N-terminal structure of TLR2-activating lipoprotein in Staphylococcus aureus.
J. Biol. Chem. 2009 Apr 3; 284(14): 9147-52.

Stübiger G, Sobal G, Widhalm K, Belgacem O, Pock K. Influence of HSA and IgG on LDL oxidation studied by size-exclusion chromatography and phospholipid profiling using MALDI tandem-mass spectrometry.
Chem. Phys. Lipids. 2011 Sep; 164(6): 563-72.

Bütikofer P, Greganova E, Liu YC, Edwards IJ, Lehane MJ, Acosta-Serrano A. Lipid remodelling of glycosylphosphatidylinositol (GPI) glycoconjugates in procyclic-form trypanosomes: biosynthesis and processing of GPIs revisited.
Biochem. J. 2010 May 27; 428(3): 409-18.

Sugiura Y, Konishi Y, Zaima N, Kajihara S, Nakanishi H, Taguchi R, Setou M. Visualization of the cell-selective distribution of PUFA-containing phosphatidylcholines in mouse brain by imaging mass spectrometry.
J. Lipid Res. 2009 Sep; 50(9): 1776-88.

Miyazaki M, Yonesige A, Matsuda J, Kuroda Y, Kojima N, Suzuki A. High-performance thin-layer chromatography/mass spectrometry for rapid analysis of neutral glycosphingolipids.
J. AOAC Int. 2008 Sep-Oct; 91(5): 1218-26.

Goto-Inoue N, Hayasaka T, Sugiura Y, Taki T, Li YT, Matsumoto M, Setou M. High-sensitivity analysis of glycosphingolipids by matrix-assisted laser desorption/ionization quadrupole ion trap time-of-flight imaging mass spectrometry on transfer membranes.
J. Chromatogr. B. Analyt. Technol. Biomed. Life Sci. 2008 Jul 1; 870(1): 74-83.

Zhu F, Cai YZ, Xing J, Ke J, Zhan Z, Corke H. Rapid identification of gallotannins from Chinese galls by matrix-assisted laser desorption/ionization time-of-flight quadrupole ion trap mass spectrometry.
Rapid Commun. Mass Spectrom. 2009 Jun; 23(11): 1678-82.

Zaima N, Hayasaka T, Goto-Inoue N, Setou M. Imaging of metabolites by MALDI mass spectrometry.
J. Oleo. Sci. 2009; 58(8): 415-9.

March RE, Li H, Belgacem O, Papanastasiou D. High-energy and low-energy collision-induced dissociation of protonated flavonoids generated by MALDI and by electrospray ionization.
Int. J. Mass Spectrom. 2007; 262: 51-66.

Cai Y, Xing J, Sun M, Zhan Z, Corke H. Phenolic Antioxidants (Hydrolyzable Tannins, Flavonols, and Anthocyanins) Identified by LC-ESI-MS and MALDI-QIT-TOF MS from Rosa chinensis Flowers.
J. Agric. Food Chem. 2005; 53: 9940-9948.

Sadanori S, Taniguchi K, Tanaka K. On-target separation of analyte with 3-aminoquinoline/α-cyano-4-hydroxycinnamic acid liquid matrix for matrix-assisted laser desorption/ionisation mass spectrometry.
Rapid Commun. Mass Spec. 2012; 26: 693-700.

Papanastasiou D, Belgacem O, Montgomery H, Sudakov M, Raptakis E. A QIT/TOF mass spectrometer combined with a Vacuum MALDI source.
Chap 19, Practical Aspects of Trapped Ion Mass Spectrometry, Vol IV. CRC Press, 2010.

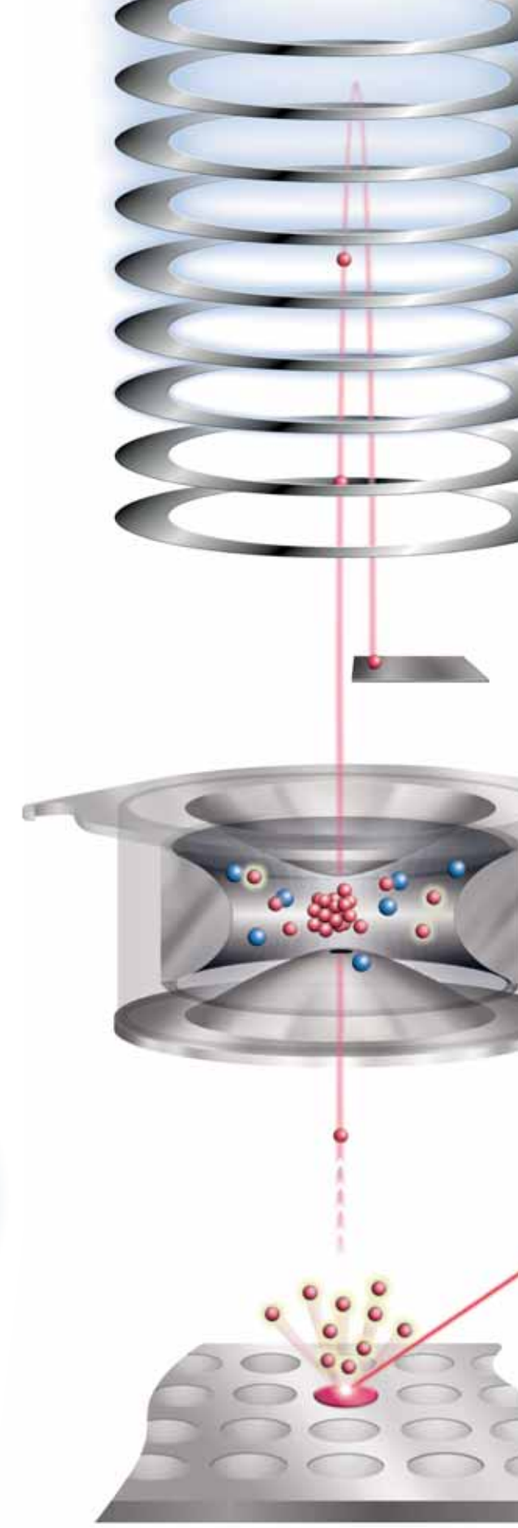

LRQ 4005852/B

Founded in 1875, Shimadzu Corporation, a leader in the development of advanced technologies, has a distinguished history of innovation built on the foundation of contributing to society through science and technology. We maintain a global network of sales, service, technical support and applications centers on six continents, and have established long-term relationships with a host of highly trained distributors located in over 100 countries. For information about Shimadzu, and to contact your local office, please visit our Web site at **www.shimadzu.com**

SHIMADZU

Kratos Analytical Ltd.
Wharfside, Trafford Wharf Road, Manchester M17 1GP, UK
Phone: +44 161 888 4400 Fax. +44 161 888 4402
URL http://www.shimadzu.com/an/